

Rapid communication

Synthetic $\text{Cu}_{0.507(5)}\text{Pb}_{8.73(9)}\text{Sb}_{8.15(8)}\text{I}_{1.6}\text{S}_{20.0(2)}$ nanowires

Galina N. Kryukova^a, Matthias Heuer^{b,*}, Gerald Wagner^b,
Thomas Doering^b, Klaus Bente^b

^a*Boriskov Institute of Catalysis, pr. Lavrentieva 5, 630090 Novosibirsk, Russia*

^b*Institute of Mineralogy, Crystallography and Materials Science, University of Leipzig, Scharnhorststr. 20, 04275 Leipzig, Germany*

Received 11 August 2004; received in revised form 18 October 2004; accepted 29 October 2004

Abstract

Nanowires of an iodine containing Pb–Sb-sulfosalts have been synthesized by chemical vapor transport. Their structure was studied using high-resolution transmission electron microscopy and X-ray powder diffraction. The lattice parameters show values equal to $a = 4.9801(4)$ nm, $b = 0.41132(8)$ nm (with two-fold superstructure), $c = 2.1989(1)$ nm and $\beta = 99.918(6)^\circ$. These parameters and the results of a multislice simulation are in good agreement with the mineral pillaite, $\text{Cu}_{0.10}\text{Pb}_{9.16}\text{Sb}_{9.84}\text{S}_{22.94}\text{Cl}_{1.06}\text{O}_{0.5}$ (space group $C2/m$, $a = 4.949(1)$ nm, $b = 0.41259(8)$ nm, $c = 2.1828(4)$ nm, and $\beta = 99.62(3)^\circ$). Microprobe and EDX analyses yielded a chemical composition of $\text{Cu}_{0.507(5)}\text{Pb}_{8.73(9)}\text{Sb}_{8.15(8)}\text{I}_{1.6}\text{S}_{20.0(2)}$ which is close to natural pillaite but contains no oxygen and iodine instead of chlorine. The structure of the investigated material is based on chains of M –S polyhedra ($M = \text{Pb}$ or Sb) typical for the architecture of sulfosalts implying iodine atoms in trigonal prismatic coordination with Pb atoms from the M –S polyhedra of neighboring chains. The [010] superstructure of the specimen was found to be unstable under electron beam irradiation with a rapid decrease of the b lattice parameter from 0.8 to 0.4 nm within 5 min.

© 2004 Elsevier Inc. All rights reserved.

Keywords: Sulfides; Nanowires; Synthesis; Structure; Transmission electron microscopy; XRD

1. Introduction

Sulfosalts form a class of complex sulfides with the general formula of $A_m B_n X_p$, where A stands for metallic elements like Pb, Ag and Cu, B represents formally trivalent, semi-metallic elements as As, Sb and Bi and X can be S and Se. In some cases sulfosalts can contain minor amounts of Cl and O. The structures of sulfosalts consist of infinite layers or rods of M –S polyhedra on the basis of the archetype structures of SnS and PbS [1]. Owing to relatively strong bonds in the chain direction, these compounds tend to grow as thin needles parallel to this direction, observed, e.g., for the minerals boulangérite [2] and jamesonite [3–5] which occur as micro needles. The stability conditions of these intermediate PbS–Sb₂S₃ phases are given in literature [6] and some

data on physical properties of iodine containing Pb–Sb–S-materials are reported [7,8]. It is highly expected that the chain-like structure of the sulfosalts may enhance the possibility for producing these materials in the nanowire-shape by relatively simple, template-free methods, such as chemical vapor transport (CVT), resublimation or rapid crystallization from the melt. Sulfosalt nanowires and nanorods bear potentialities for applications in electronics, as their structures and semiconducting properties are derived from archetypes such as CuS, Sb₂S₃ and PbS which have band gaps between 1.2 and 1.7 eV [9–14]. It is important to note that superstructures possibly responsible for the electronic effects have been observed in natural and synthetic Pb–Sb-sulfosalts [5,15–17]. Recently, we reported that nanowires of Pb–Sb-sulfides with diameters of ca. 100 nm could be synthesized from the melt [18]. Scanning electron microscopy (SEM) gave evidence that this material solely occurs as bundles of

*Corresponding author. Fax: +49 341 973 6299.

E-mail address: heuer@rz.uni-leipzig.de (M. Heuer).

parallel-intergrown individual nanowires. Using these facts and because natural halogen-bearing sulfosalts such as pillaite [19], pellouxite [20], dadsonite [22] and ardaite [23] as well as the halogen-free mineral boulangerite [21] reveal needle-like morphology, we tried to apply the CVT procedure with iodine as transport agent to grow different Pb–Sb-sulfosalts in the form of nanowires. In this paper an XRD-study as well as HRTEM analysis along with computer simulation of HRTEM images were used to examine the structural arrangement of the ternary sulfosalt and to provide a structural model of this compound.

2. Experimental

CVT synthesis was performed in 10 mm diameter and 75 mm long silica tubes with I_2 as transport agent (0.3 mg I_2 /mL) in a two-zone furnace with a temperature gradient ranging from 456 to 380 °C. Initially it was intended to recrystallize different Pb–Sb-sulfosalts in the form of nanowires or nanorods using CVT. Therefore in one experiment natural jamesonite, $FePb_4Sb_6S_{14}$, from Wolfsberg (Harz, Germany) was used as starting material. Since the source was a massive piece of intergrown needles, there was no risk of mixing the starting material with the products, which were separately growing needles.

After 10 days the ampoules were cooled down at the precursor side by water to condensate I_2 and to avoid contamination of the transported products and grown needles, respectively.

The XRD-data were collected using Cu $K\alpha$ -radiation ($\lambda = 1.541874 \text{ \AA}$) on a XRD3000-diffractometer (Seifert) in a range of $2\theta = 12\text{--}90^\circ$ with a step size of 0.02° and a counting time of 20 s. The device operates in Bragg-Brentano-Geometry with a secondary monochromator (graphite (002)) and a scintillation detector. For the profile calculation and the determination of the lattice parameters, the program FULLPROF [26] was used.

Study of the specimens' morphology has been carried out with the use of Zeiss DSM 640 scanning electron microscope (SEM) operating at 15 kV/20 μ A. The chemical composition of the samples was determined by electron probe microanalysis using Cameca SX 100 (15 kV/20 nA, standards: synthetic PbS , Sb_2S_3 or $InSb$) and by energy-dispersive X-ray analysis in a transmission electron microscope. HRTEM examinations were carried out in a Philips CM200 transmission electron microscope operated at 200 kV. For HRTEM analysis the specimen was placed between GaAs-wafers used as dummy materials and cut across and along the wires length followed by mechanical polishing and etching by Ar^+ ions using an acceleration voltage of 4 kV, a beam current of 0.5 mA and beam incident angle of 13° . HRTEM image simulations were performed

using MacTempas program based on the multislice algorithm [24].

3. Results

The SEM image of the synthesized specimen (Fig. 1) shows bundles consisting of several wires with sizes of 300 nm in diameter and up to 80 μ m in length, respectively. In a TEM bright field image of such bundle in a cross section (projection in [010]-direction), individual nanowires with diameters down to 200 nm become visible (Fig. 2). Microprobe and EDX analyses on the CVT-grown material yielded a formula of $Cu_{0.507(5)}Pb_{8.73(9)}Sb_{8.15(8)}I_{1.6}S_{20.0(2)}$. This unbalanced formula may be explained by the following facts. On the one hand the measurement of iodine has high uncertainties due to overlaps of the lines in the measured spectra and on the other hand an evaporation of iodine from the material during specimen irradiation within the microprobe is possible. Therefore, one can expect that the iodine content is higher than measured. Compared to natural pillaite, the CVT material contains no oxygen, iodine instead of chlorine and has one formula unit Sb_2S_3 less than the mineral. This suggests that the structures of the iodine containing material and natural pillaite are very similar but not exactly the same and reflects the chemical variability of sulfosalts. Furthermore, this result was unexpected since a natural jamesonite was the starting material in the CVT experiment. A reinvestigation of the initial material by electron microprobe analysis revealed that the mineral sample from Wolfsberg (Harz, Germany) consists mainly of jamesonite with a composition of $Fe_{0.873(8)}Pb_{4.01(4)}Sb_{6.12(6)}S_{13.8(2)}$ and minor amounts of a further copper-containing phase with a composition

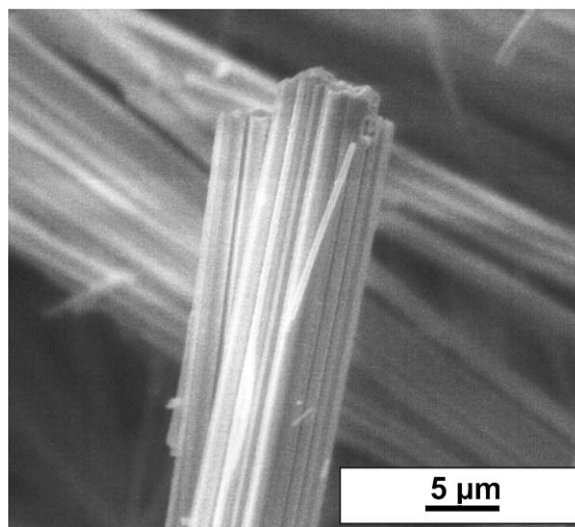


Fig. 1. SEM micrograph of a bundle of CVT-grown $Cu_{0.507(5)}Pb_{8.73(9)}Sb_{8.15(8)}I_{1.6}S_{20.0(2)}$.

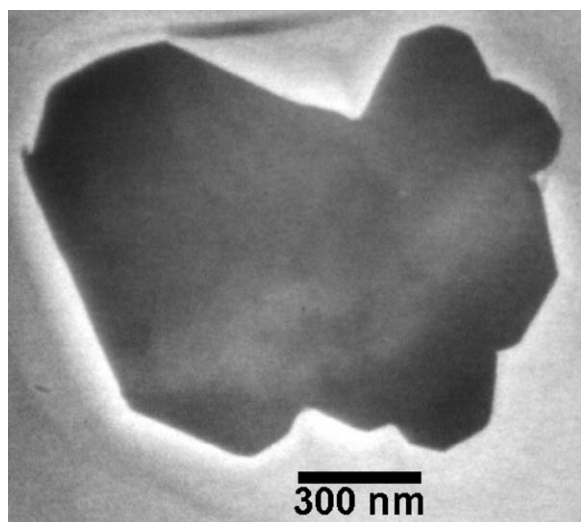


Fig. 2. TEM bright field image of a bundle of individual nanowires with diameters down to 200 nm in cross section (projection in [010]-direction).

of $\text{Ag}_{0.462(4)}\text{Cu}_{0.056(2)}\text{Pb}_{1.69(2)}\text{Sb}_{2.08(2)}\text{S}_{5.0(5)}$ (possibly owyhecite). Thus the resulting composition of $\text{Cu}_{0.507(5)}\text{Pb}_{8.73(9)}\text{Sb}_{8.15(8)}\text{I}_{1.6}\text{S}_{20.0(2)}$ can be explained subsequently by different transport rates of the elements during the CVT process and the partial incorporation of the transport agent iodine.

HRTEM images viewed across and along an individual wire together with their selected area electron diffraction (SAED) patterns are given in Figs. 3 and 4, respectively. The structure across the wire reflects a rod-like nature of the material with zigzag chains forming a specific closed motif of the twisted, irregular rhomb shape (Fig. 3). Distance between the centers of two adjacent rhombi is ca. 2.15 nm. At the image taken in [100] projection one can see doubled rows of closely spaced dots with a spacing between them equal to 0.4 nm that is typical of sulfides structure in the chain direction. Periodicity across the rows exhibits a value of ca. 2.1 nm (two little arrows).

The examination of a SAED pattern taken from a cross section of the wire (see inset in Fig. 4) revealed an angle of $99.5(1)^\circ$ between the [001] and the [100] direction indicating monoclinic symmetry. Besides, the atomic radius of iodine is too big (about 0.220 nm, [28]) and therefore it could not be simply exchanged with a smaller sulphur ion (atomic radius is 0.184 nm, [28]) within the chain. These circumstances are similar to the structure of the mineral pillaite ($\text{Cu}_{0.10}\text{Pb}_{9.16}\text{Sb}_{9.84}\text{S}_{22.94}\text{Cl}_{1.06}\text{O}_{0.5}$) which hosts a big chlorine ion, crystallizes in the monoclinic space group $C2/m$, and has lattice parameters of $a = 4.949(1)$ nm, $b = 0.41259(8)$ nm, $c = 2.1828(4)$ nm and $\beta = 99.62(3)^\circ$ [19]. It should be noted that values of lattice periodicities observed in the experimental HRTEM micrographs as well as the angle between rows of diffraction spots in the

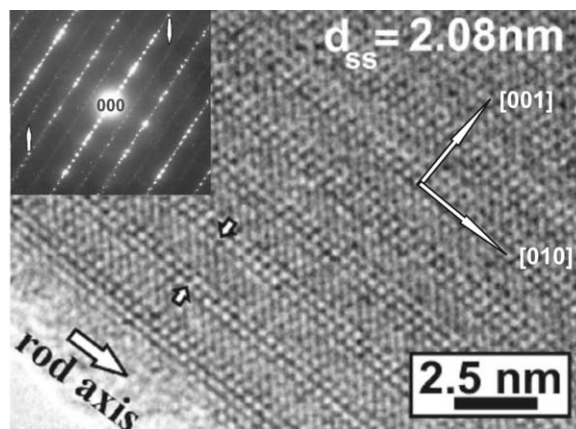


Fig. 3. HRTEM image and SAED pattern (inset) of the structure of an individual single crystalline nanowire viewed along [100] and across wire direction. Arrows in SAED pattern mark weak additional reflections. Periodicity across the rows exhibits a value of 2.08 nm (two little arrows).

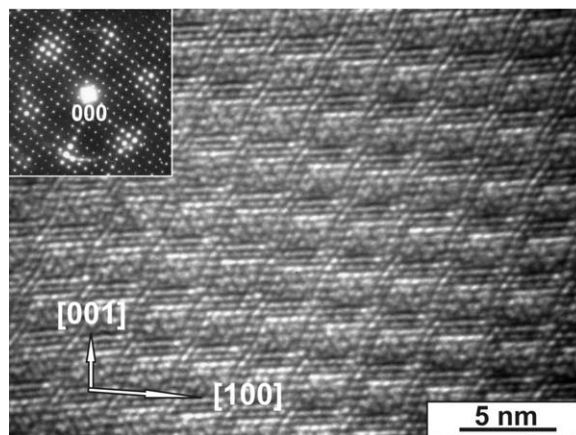


Fig. 4. HRTEM image and SAED pattern (inset) of the structure of an individual single crystalline nanowire viewed along [010] and along the wire direction.

SAED patterns with $a = 5.00(1)$ nm, $b = 0.40(1)$ nm, $c = 2.10(1)$ nm and $\beta = 99.5(1)^\circ$ are very close to these cell parameters. Image simulations gave evidence that defocus conditions and specimen thickness strongly affect the contrast observed in the experimental HRTEM micrographs. Hereby a model was used which is derived from pillaite by replacing the chlorine atoms by iodine and deleting the oxygen. However, with the experimental defocus equal to -87.5 nm and at a crystal thickness of 12 nm we obtained reasonably good fitting (Fig. 5) between experimental and calculated images. For comparison Fig. 6 gives a structure projection along [010] direction. In this model iodine atoms are coordinated in the trigonal prisms by adjacent Pb atoms. As evident from the comparison of experimental and theoretical images given in Fig. 5, bright spots represent the sulphur atomic columns, weak spots at the corners

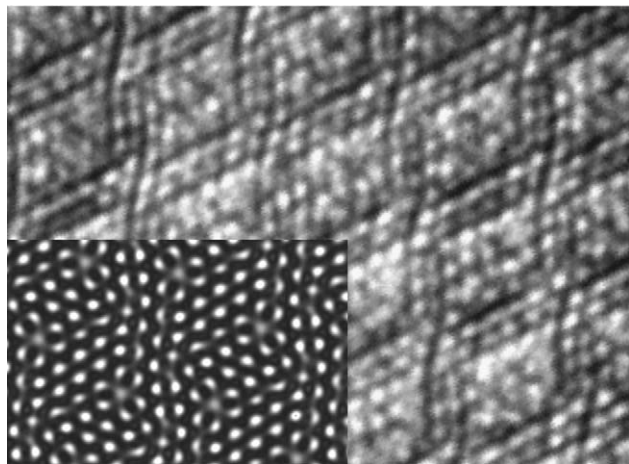


Fig. 5. Calculated and experimental HRTEM images of the $\text{Cu}_{0.507(5)}\text{Pb}_{8.73(9)}\text{Sb}_{8.15(8)}\text{I}_{1.6}\text{S}_{20.0(2)}$ structure in [010] view direction for a defocus value $\Delta f = -87.5$ nm and a thickness $t = 12$ nm (long edge of figure approximately 20 nm).

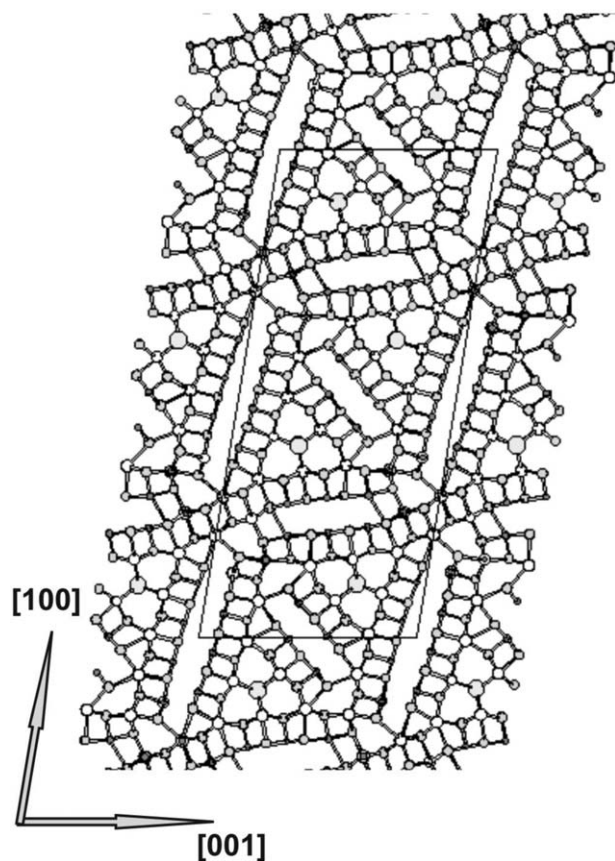


Fig. 6. Schematic representation of the $\text{Cu}_{0.507(5)}\text{Pb}_{8.73(9)}\text{Sb}_{8.15(8)}\text{I}_{1.6}\text{S}_{20.0(2)}$ structure viewed along [010] direction. The model is derived from structure data of natural pillaite [19] replacing the chlorine atoms by iodine and deleting the oxygen. The S atoms are depicted by the small light grey circles, I atoms by the largest light grey circles, Sb atoms by the smallest dark grey circles, and the Pb atoms by the medium white circles; unit cell is marked by bold line.

of the distorted rhomb reflect the position of iodine atoms and all heavy atoms (Sb, Pb and/or Cu) are not imaged in this case. Copper atoms are suggested to replace Pb or Sb by heterotopic substitution [25] or to occupy tetrahedral coordinated vacancies [19].

An important observation stems from the fact that the nanowire grows along the b -axis that is the shortest axis of the proposed structure (long expansion of the wire is marked by arrow in Fig. 3). Furthermore, a superstructure with a doubled b lattice parameter (~ 0.8 instead of ~ 0.4 nm) was observed for the CVT-grown material expressed as additional reflections in the SAED pattern and marked by arrows in the inset of Fig. 3. It is important to note that this experimental fact is in line with XRD investigations on pillaite single crystals [26,29]. In the first minutes of a HRTEM experiment these additional diffraction spots, weak but still recognizable, are present in SAED pattern and indicate the ordering in the nanowire structure. After 5 min irradiation of the specimen these weak reflections disappear along with a decrease of the b lattice parameter from 0.8 to 0.4 nm. This easy transformation of the structure upon the beam leads to the intriguing chance that by assembling alternating areas with ordered and disordered arrangements along the wire, it might be possible to control the alternation of electronic properties of the sulfosalts nanorods.

Furthermore an XRD study supports the close structural relationship between the investigated material and pillaite. To simulate the X-ray pattern, the structure model of pillaite [19] was used in a modified form, i.e., the chlorine atom was changed into iodine and the oxygen was excluded. It was tried to carry out a Rietveld refinement using FULLPROF [27], but due to the excessive peak overlap with 2138 reflections in a range from $2\theta = 12\text{--}90^\circ$ it was not possible to obtain a stable convergence of the atom coordinates, site occupancies and thermal displacement parameters. Nevertheless, the lattice and the profile parameters could be refined (Table 1) assuming a polynomial background and a

Table 1

Cell and profile parameters of CVT grown $\text{Cu}_{0.507(5)}\text{Pb}_{8.73(9)}\text{Sb}_{8.15(8)}\text{I}_{1.6}\text{S}_{20.0(2)}$ resulting from a refinement on powder XRD data

Cell parameters:	Half width parameters:
$a = 4.9801(4)$ nm	$U = 1.357329(1)$
$b = 0.41132(8)$ nm	$V = -0.003075(1)$
$c = 2.1989(1)$ nm	$W = -0.022437(1)$
$\beta = 99.918(6)^\circ$	
Scale factor:	Background parameters:
osf = 0.00000072(2)	$P0 = 273(5)$
	$P1 = -202(10)$
Preferred orientation [010]:	$P2 = 440(12)$
$G1 = 0.56(2)$	$P3 = -644(31)$
	$P4 = 304(20)$

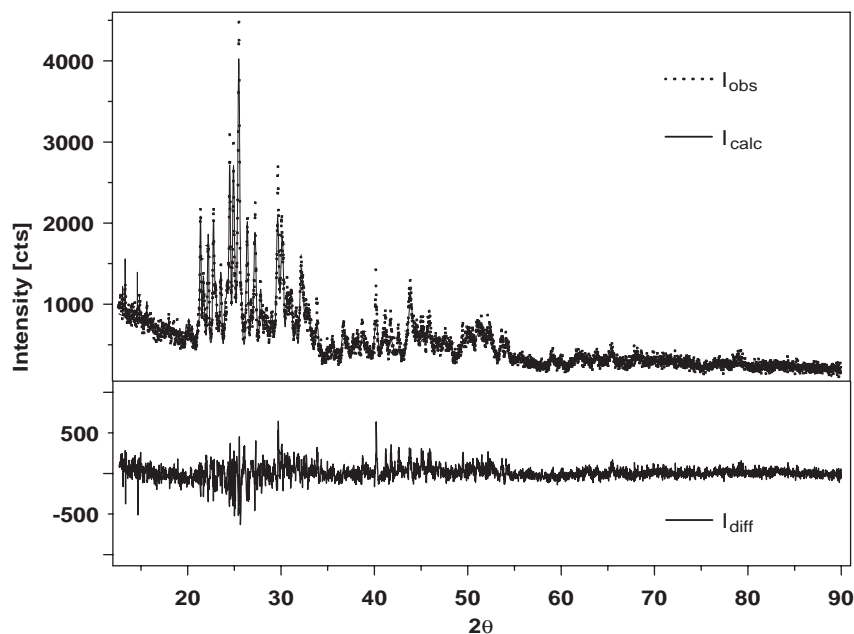


Fig. 7. Comparing plot of XRD data measured at CVT grown $\text{Cu}_{0.507(5)}\text{Pb}_{8.73(9)}\text{Sb}_{8.15(8)}\text{I}_{1.6}\text{S}_{20.0(2)}$ and calculated using a structure model derived from natural pillaite [19]. $R_{\text{Bragg}} = 12.7\%$, $R_{\text{p}} = 11.3\%$, $I_{\text{diff}} = I_{\text{obs}} - I_{\text{calc}}$.

preferred orientation of the [010] elongated needles. The resulting calculated pattern is very similar to the measurement, shown in Fig. 7 and it matches with a Bragg R -factor of 12.7% and a R_{p} of 11.3%. It is still unsolved how the structural differences between the investigated material and pillaite can be explained, i.e., the lower Sb_2S_3 -content in the CVT material.

Resuming the (HR)TEM, EDX, WDX and XRD results it can be demonstrated that the investigated material is very similar to natural pillaite but not exactly the same. It is a task for forthcoming X-ray studies with single crystals to explore the structural details and differences.

4. Conclusions

Using HRTEM, XRD, electron microprobe and EDX measurements, we have shown that the CVT-grown nanowires of $\text{Cu}_{0.507(5)}\text{Pb}_{8.73(9)}\text{Sb}_{8.15(8)}\text{I}_{1.6}\text{S}_{20.0(2)}$ composition represent a novel iodine containing Pb–Sb-sulfosalt with following cell parameters: $a = 4.9801(4)$ nm, $b = 0.41132(8)$ nm with twofold superstructure, $c = 2.1989(1)$ nm, $\beta = 99.918(6)^\circ$. The proposed structure model is close to the chlorine-containing mineral pillaite, $\text{Cu}_{0.10}\text{Pb}_{9.16}\text{Sb}_{9.84}\text{S}_{22.94}\text{Cl}_{1.06}\text{O}_{0.5}$ (space group $C2/m$, $a = 4.949(1)$ nm, $b = 0.41259(8)$ nm, $c = 2.1828(4)$ nm, $\beta = 99.62(3)^\circ$), for which a superstructure is reported too. The examination of the powder XRD data supports the close structural relationship between the investigated material and pillaite. Undoubtedly, further work is intended to

synthesize isolated nanowires of the same composition and to perform a structural analysis of the material using X-ray diffraction by single crystals. Further investigation should also verify, whether the material will show quantum size effects and if the electronic properties of this compound can be tuned by creating the sequences of ordered and disordered regions along the wires.

Acknowledgments

The financial support from the Deutsche Forschungsgemeinschaft under Be 1088/20-1 within the ‘‘Forschergruppe’’ FOR 522 is greatly appreciated.

References

- [1] E. Makovicky, in: S. Merlino (Ed.), EMU Notes in Mineralogy, Vol. 1: Modular Aspects of Minerals, Eötvös University Press, Budapest, 1997.
- [2] A. Skowron, I.D. Brown, Acta Crystallogr. B 50 (1994) 524.
- [3] S. Hanson, A. Falster, W. Simmons, Rocks Minerals 67 (1992) 113.
- [4] N. Nizeki, M.J. Buerger, Z. Kristallographie (1957) 161.
- [5] L.G. Berry, University of Toronto studies, Geological Series 48 (1943) 9.
- [6] B. Salanci, N. Jb. Miner. Abh. 135 (1979) 315.
- [7] I.D. Turyanitsa, I.M. Migolnits, B.M. Koperles, I.F. Kopinets, Izv. Akad. Nauk SSSR, Neorgan. Mater. 18 (1974) 8.
- [8] M.P. Lisitsa, I.D. Turyanitsa, I.V. Fekeshgazi, Phys. Stat. Sol. B 146 (1988) 723.
- [9] D. Chen, K. Tang, G. Shen, J. Sheng, Z. Fang, X. Liu, H. Zheng, Y. Quian, Materials Chem. Phys. 82 (2003) 206.

- [10] H. Dittrich, K. Herz, *Institute of Physics Conference Series (ICTMC)* 152 (1998) 293.
- [11] H. Hanmei, M. Maosong, Y. Baojun, Z. Xuanjun, L. Qiaowei, Y. Weichao, Q. Yitai, *J. Crystal Growth* 258 (2003) 106.
- [12] Y. Dabin, W. Debao, M. Zhaoyu, L. Jun, Q. Yitai, *J. Mater. Chem.* 12 (2002) 403.
- [13] J. Chen, S.Z. Deng, J.C. She, N.S. Xu, W. Zhang, X. Wen, S. Yang, *J. Appl. Phys.* 93 (2003) 1774.
- [14] L. Bakueva, et al., *Appl. Phys. Lett.* 82 (2003) 2895.
- [15] H. Dornberger-Schiff, *Chemie d. Erde B* 22 (1962) 78.
- [16] W. Mumme, *N. Jb. Miner. Mh.* 11 (1989) 498.
- [17] G.H. Moh, K. Bente, M. Meier-Salimi, *N. Jb. Miner. Abh.* 163 (1991) 197.
- [18] M. Heuer, G. Wagner, T. Döring, K. Bente, G. Kryukova, *J. Cryst. Growth* 267 (2004) 745.
- [19] A. Meerschaut, P. Palvadeau, Y. Moelo, P. Orlandi, *Eur. J. Miner.* 13 (2001) 779–790.
- [20] P. Palvadeau, A. Meerschaut, P. Orlandi, Y. Moelo, *Eur. J. Miner.* 5 (2004) in press.
- [21] V.V. Breskovska, N.N. Mozgova, N.S. Bortnikov, A.I. Tsepin, *Dokl. Bolgarskoi Akad. Nauk.* 32 (1979) 1.
- [22] V.V. Kostov, J. Macinek, *Eur. J. Miner.* 7 (1995) 1007.
- [23] V.V. Kostov, R. Petrova, J. Macinek, *Eur. J. Miner.* 9 (1997) 1191.
- [24] M.J. Hytch, E. Schoeck, R. Kilaas, *Ultramicroscopy* 74 (1998) 131.
- [25] K. Bente, V. Kupcik, H. Siebert, *Fortschr. Mineral.* 61 (1983) 20.
- [26] Y. Moelo, private communication.
- [27] J. Rodriguez-Carvajal, “FULLPROF: A Program for Rietveld Refinement and Pattern Matching Analysis”, Abstracts of the Satellite Meeting on Powder Diffraction of the XV Congress of the IUCr, Toulouse, France, 1990, p. 127.
- [28] R.D. Shannon, *Acta Cryst. A* 32 (5) (1976) 751–767.
- [29] P. Orlandi, Y. Moelo, A. Meerschaut, P. Palvadeau, *Eur. J. Miner.* 13 (3) (2001) 605–610.